

Original Research

PKM2 in Canine Mammary Tumors: Parallels to Human Breast Cancer

Hyo-Ju Lee,¹ Hyo-Jeong Han,^{1,2} Ji-Young Lee,^{1,2} and Woo-Chan Son^{1,2*}

PKM2 is a pyruvate kinase isoform that is the final and rate-limiting step in aerobic glycolysis in tumor cells. Increased expression of PKM2 has been detected in human cancers. The present study examined the expression of PKM2 in canine mammary tumors and assessed its prognostic significance. Paraffin sections of 5 adenomas, 67 carcinomas, and 5 samples of nonneoplastic hyperplasia from 77 dogs, aged 8 to 18 y, were evaluated. Significantly higher levels of PKM2 were detected among the carcinomas compared with all other tissues examined. The level of PKM2 expression in carcinoma tissue correlated positively with the tumor grade. These findings suggest that PKM2 may have a similar role in canine mammary tumors to its role in human breast cancer. As such, canine mammary tumors may be useful models for studies focused on the progression of human neoplastic disease.

Abbreviations: CMTs, canine mammary tumors; HIF1, hypoxia-inducible factor-1; HIF1 α , hypoxia-inducible factor-1 α

DOI: 10.30802/AALAS-CM-20-000013

Canine mammary tumors (CMTs) are currently being assessed for their use as a model for investigating the pathogenesis and prognosis of human breast cancer.¹ Dogs with spontaneously occurring neoplasms are a particularly valuable resource for modeling human cancers, because the breast cancers of both species have similar biologic behaviors, histopathologic characteristics, and metastatic patterns.²⁸ Previous studies have shown that biomarkers of human cancer can be detected in CMTs, including hypoxia-inducible factor-1 (HIF1) and hypoxia-inducible factor-1 α (HIF1 α), with similar clinical implications.¹⁷ Consequently, CMTs may be an appropriate model for exploring mechanisms associated with the pathogenesis of human breast cancer.

HIF1 is a heterodimeric transcription factor that includes an O₂-regulated HIF1 α subunit. HIF1, has been implicated in advanced human cancers and is a key regulator of transcriptional responses to hypoxia. HIF1 is activated in many cancer types and has been identified as a driving force behind cancer progression.²³ HIF1 activates transcription of genes that encode proteins mediating angiogenesis, invasion, metastasis and the shift from oxidative to glycolytic metabolism.

In tumor metabolism, most cancer cells consume more glucose and produce more lactate than do their nonneoplastic counterparts. This phenomenon, known as the Warburg effect, suggests adaptations and mechanisms underlying tumor cell growth.⁹ While normal cells maximize adenosine triphosphate production via mitochondrial oxidative phosphorylation of glucose, cancer cells are somewhat less dependent on this pathway.³ Pyruvate kinase (PK) catalysis the final step in aerobic glycolysis. The human genome encodes 2 distinct PK genes,

PKLR and PKM. Isomers PKM1 and PKM2 are encoded by the same gene but are generated by differential splicing. PKM2 expression is associated with glucose uptake, lactate production and decreased O₂ consumption in cancer cells.²⁶ Likewise, PKM2 expression results in elevated levels of HIF1 binding to hypoxia response elements in target genes and promotes the shift from oxidative phosphorylation to glycolytic metabolism.²⁹

In this study we evaluated PKM2 expression in CMTs, which are among the most frequent malignancies characterized in canine species. Moreover, given the similarities in epidemiologic and pathologic features shared by CMT and human breast cancer, we assessed the clinical significance of PKM2 expression in CMT.

Materials and Methods

Tumor sample selection. Mammary tumor tissues were isolated from 76 dogs from 5 participating veterinary clinics in Seoul, Korea, during the years 2014 and 2015. All tissues were fixed in 10% buffered formalin and embedded in paraffin. A single pathologist evaluated all hematoxylin and eosin-stained slides.

Immunohistochemistry. Sections from paraffin-embedded tissue blocks of canine mammary gland tumor were cut to 3 μ m and mounted on glass slides. Immunohistochemistry was carried out using a Benchmark XT automated slide preparation system (Ventana Medical Systems, Tucson, AZ). Deparaffinization, epitope retrieval, and immunostaining were performed according to the manufacturer's instructions by using cell conditioning solutions (CC1) and the BMK ultraView diaminobenzidine (DAB) detection system (Ventana Medical Systems). Antibodies used for immunohistochemical staining included anti-PKM2 (1:400 dilution, cat. number 4053; Cell Signaling, Danvers, MA.) and anti-HIF α (1:100 dilution, cat. no. NB 100 to 134; Novus Biologicals, Littleton, CO.). Positive signals were amplified with ultraView copper, and sections

Received: 21 Feb 2020. Revision requested: 27 Mar 2020. Accepted: 21 Apr 2020.

¹Department of Pathology, University of Ulsan College of Medicine, Asan Medical Center, Seoul, Korea; ²Asan Institute for Life Sciences, Asan Medical Center, Seoul, Korea

*Corresponding author. Email: wacson@amc.seoul.kr

were counterstained with hematoxylin and bluing reagent. Automated immunohistochemistry to detect expression of HIF1 α was performed in a Benchmark XT staining module (Ventana Medical Systems) on 3- μ m-thick canine tumor sections with the rabbit antihuman polyclonal antibody (NB 100 to 134; Novus Biologicals). Briefly, after deparaffinization, heat-mediated antigen retrieval and inactivation of endogenous peroxidase, the primary antibody was applied in manufacturer-supplied antibody diluent for all samples. Detection was performed with the OptiView DAB IHC Detection Kit with signal amplification (a gift from Ventana Medical Systems) following the manufacturer's instructions.

Evaluation and quantification of the immunohistochemical reaction. Microscopic examination was used to determine the tumor grade of each of the carcinomas based on the Elston and Ellis modification of the Bloom-Richardson method.¹⁰ The tumor received a score of 0, 1, 2, or 3 based on 3 parameters: formation of tubules (normal, weak, slight, and moderate), polymorphism of cell nuclei (normal, weak, slight, and moderate), and number of mitotic figures per 10 microscope fields at a magnification of $\times 400$ (0 to 7, 8 to 16, and greater than or equal to 17). The sum of the points allowed us to distinguish between 3 tumor grades (G): G1 (0 to 5 points), G2 (6 to 7 points), and G3 (8 to 9 points). For PKM2 and HIF1 α , the intensity, percentage, and localization of the immunohistochemical detection in the cells of each tumor were recorded. Healthy canine mammary tissues from dogs without mammary or lobular hyperplasia were used as positive controls and staining with the omission of the primary antibody performed as a negative control. The intensity and percentage of positively stained cells were counted in 10 high-powered fields ($\times 400$), and the intensity of staining was recorded as 0 to 3 points for negative, weak, moderate and strong staining, respectively. The degree of the cytoplasmic PKM2 and nuclear HIF1 α expression was scored from 0 to 300 using the Q score, which is obtained by multiplying the intensity by the percentage of positive cells (maximum = 300).⁵

Tissue ribonucleic acid (RNA) extraction and cDNA synthesis. Total RNA was extracted from approximately 100 mg of canine breast tissue using Hybrid-RTM according to the manufacturer's instructions (GeneAll Biotechnology, Korea). Samples were homogenized with a TissueLyser II (Qiagen, Germany) in a 2.0-mL microfuge tube using 1 mL of TRIzol (Invitrogen) per 100 mg of tissue. RNA yields and purity were determined by measuring the absorbance at 260 and 280 nm using a NanoDrop ND-1000 UV-Vis Spectrophotometer (Thermo Fisher Scientific, Czech Republic). All samples had an A260/A280 absorbance ratio greater than 1.8. The quality of the RNA was confirmed by agarose gel electrophoresis and its integrity was checked with a 3':5' assay according to published instructions.¹⁸ To avoid contamination with genomic DNA, 10 μ g of RNA was treated with DNase I (NEB) for 20 min at 37 $^{\circ}$ C, followed by heat inactivation for 10 min at 75 $^{\circ}$ C and dilution to a concentration of 0.2 μ g/ μ L. RNA was stored at -80 $^{\circ}$ C until further analysis. First-strand synthesis of mRNA was carried out using ProtoScript II reverse transcriptase and random hexamers (or oligo-dT for the 3':5' assay) using the manufacturer's protocol (Enzymomics). After initial heat denaturation of 1 μ g of total RNA (65 $^{\circ}$ C for 5 min), the reactions (20 μ L) were incubated for 10 min at 25 $^{\circ}$ C, for 50 min at 42 $^{\circ}$ C, and for 15 min at 75 $^{\circ}$ C.

For the synthesis of cDNA from miRNAs and small RNAs, the reaction mixture included stem-loop oligonucleotides specific for each miRNA and sno202 or specific reverse primers for sno234 and U6.⁶ First-strand synthesis was carried out using ProtoScript II reverse transcriptase. After initial heat denaturation (65 $^{\circ}$ C for 5 min), total RNA was used in reactions (10 μ L

Table 1. Primer sequences used for real-time qPCR

Animal	Name	Sequence (5' to 3')
Canine	PKM2	F: GAGTTCGGAGGTTTGATGAG
		R: CATCTTCTGAGCAAGGAAGAC
Canine	HIF1 α	F: GACCCGGCACTCAATCAAGA
		R: ATCCATTGATTGCCCCAGCA
	GAPDH	F: ACTACATGGTGGTGTACATGTTCCA
		R: CTCCTGGAAGATGGAGATGG

were incubated for 30 min at 16 $^{\circ}$ C, for 30 min at 42 $^{\circ}$ C, and for 15 min at 75 $^{\circ}$ C. The cDNA obtained was diluted (5 \times , 50 \times for target RNAs and 10 \times or 10 $^5\times$ for analysis of glyceraldehyde-3-phosphate dehydrogenase [GAPDH]) prior to performing quantitative real-time polymerase chain reaction (qPCR). All cDNA samples were stored at -20 $^{\circ}$ C prior to their use in the qPCR assay.

Primer design and qPCR. The primers for mRNA normalization were obtained from PrimerBank (<http://pga.mgh.harvard.edu/primerbank>) and were designed using Primer3 software,²⁴ or had been described in previous reports. For mRNA normalization, the reverse primer used was universal^{6,18} and the forward primers were designed using OligoCalc (<http://biotools.nubic.northwestern.edu/OligoCalc.html>).¹⁴ All primers were synthesized by Bioneer, Daejeon, Korea. The specificity of the primers was checked using the National Center for Biotechnology Information Blast tool, and the reaction conditions were optimized by adjusting the primer concentrations. The primer sequences (with their corresponding bibliographic references) are listed in Table 1.

The qPCR analyses were performed in a Step One Plus (Applied Biosystems, Foster City, CA.) real-time PCR system using SYBR Green I detection in a final volume of 20 μ L. The reaction mixture consisted of components from the qPCR Core kit for SYBR Green I (Applied Biosystems) as specified by the manufacturer, both forward and reverse primers and 5 μ L of diluted cDNA. The same batch of diluted cDNA (5 μ L, corresponding to 50 ng of reverse-transcribed RNA) was subjected to qPCR to amplify all candidate genes for mRNA normalization, as well as the target gene. Five microliters of the respective cDNAs were used for the qPCR analysis of each mRNA. The PCR reactions were initiated by a denaturation step of 10 min at 95 $^{\circ}$ C, followed by 40 cycles of amplification, which were performed according to the following thermocycling profiles: denaturation for 10 s at 95 $^{\circ}$ C and annealing and extension for 40 s at 60 $^{\circ}$ C. Fluorescence data were acquired during the final step. A dissociation protocol with a gradient (0.5 $^{\circ}$ C every 30 s) from 65 $^{\circ}$ C to 95 $^{\circ}$ C was used to confirm the specificity of the qPCR reaction for the single target and to assess the presence of primer dimers. Gene-specific amplification was confirmed by a single peak in the melting curve analysis.

Data analysis. To select a suitable reference gene for data normalization, the stability of the mRNA expression of each gene was statistically analyzed with 3 freely available Microsoft Excel-based software packages: geNorm [<http://medgen.ugent.be/~jvdesomp/genorm/>] (Vandesompele), NormFinder [<http://moma.dk/normfinder-software>], and BestKeeper [<http://gene-quantification.com/bestkeeper.html>]. For geNorm and NormFinder, the raw Cq values were transformed into relative quantities (the required data input format). The maximum expression level (the lowest Cq value) of each gene was used as a control and was set to a value of 1. Relative expression levels were then calculated from Cq values using the

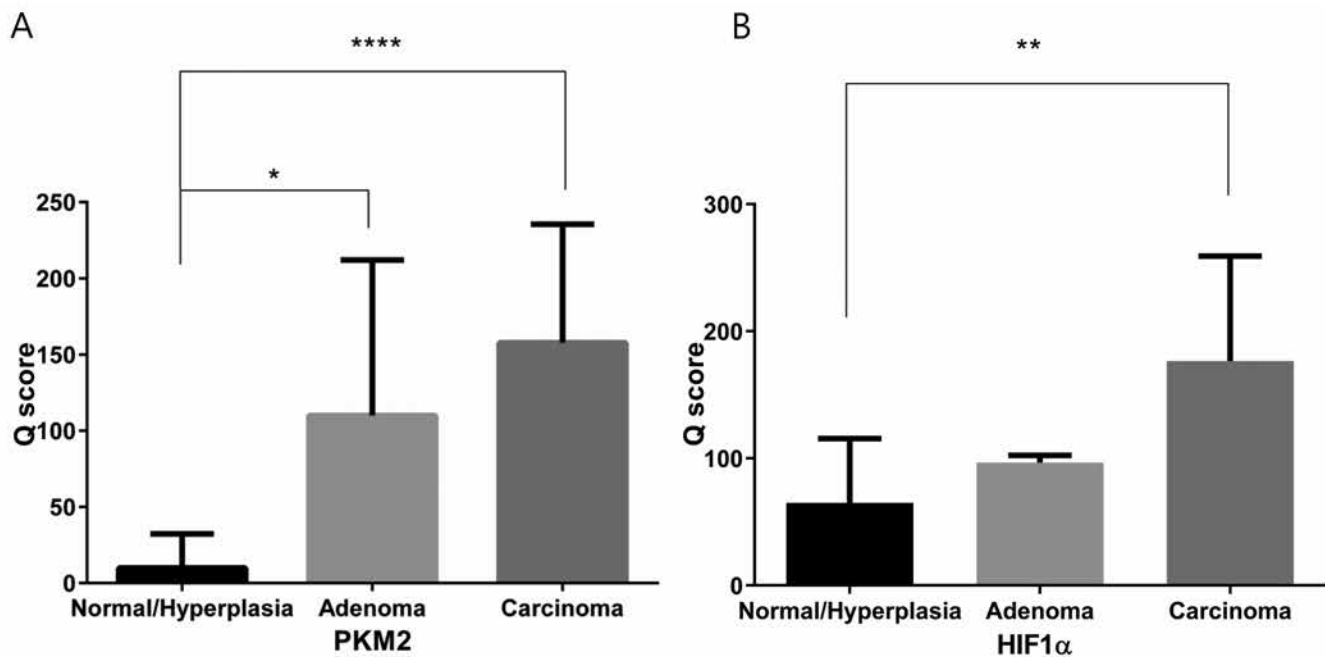


Figure 1. Bar graph displaying the Q scores of PKM2 and HIF1 α expression in canine mammary tumor tissue. (A). PKM2 expression in canine mammary carcinoma. (B). HIF1 α expression in canine mammary carcinoma. *, $P < 0.03$, **, $P < 0.002$, ****, $P < 0.0001$.

formula: $2\lambda(-\Delta Cq)$, in which ΔCq represents each corresponding Cq value – minimum Cq value.²¹ The data obtained were further analyzed with geNorm and NormFinder. BestKeeper analyses were based on untransformed Cq values. For consensus ranking of all candidate reference genes, the geometric mean of the ranks from these 3 analyses was determined.

Statistical analyses. Data are presented as the mean \pm SEM. Statistically significant differences were assessed using the Student t test or χ^2 test, and $P < 0.05$ was considered significant. Statistical analyses were performed using GraphPad Prism version 6 (GraphPad, San Diego, CA).

Results

Tumor characteristics. Our collection of CMTs included 25 complex carcinomas, 20 mixed carcinomas, 22 other types of carcinomas, 5 adenomas and 5 normal or nonneoplastic hyperplasia samples. The ages of the 77 dogs ranged from 8 to 13 y. The mean of the long axis of the tumors was 4.1 ± 2.5 cm (ranging from 0.5 to 11 cm).

Comparison of PKM2 and HIF1 α expression in normal mammary gland and cancer cells. The neoplastic cells displayed variable expression of PKM2 that ranged from weak to strong. The normal mammary cells in tissue located near the tumor and the nonneoplastic hyperplastic cells showed weak to no reactivity with the anti-PKM2 antibody. Thus, the Q scores of PKM2 of the neoplastic cells were significantly higher ($P < 0.0001$) than those of their normal counterparts (Figure 1 A). PKM2 protein was detected in both mammary adenomas and carcinomas. None of the adenomas that we evaluated had a level of PKM2 expression that exceeded an intensity score of 100. However, more than 20% (14 of 67) of the carcinomas demonstrated PKM2 expression intensity of 0.5 to 1.0, over 30% (23 of 67) had an intensity of 1.5 to 2.0, and over 40% (27 of 67) had levels as high as 2.5 to 3.0.

Similar to PKM2, minimal expression of HIF1 α was detected in normal and hyperplastic nonmalignant cells and in adenoma tissues, but elevated levels were detected in the carcinomas. Furthermore, the expression of HIF1 α was generally higher in

carcinomas than in adenomas (Figure 1 B). All (100%) of the normal/hyperplastic and adenoma tissues examined displayed a HIF1 α expression intensity of 0 or 1. By contrast, among the carcinomas, over 35% (24 of 67) displayed a HIF1 α intensity of 0 to 1, 31% (21 of 67) displayed an intensity of 1.5 to 2, and over 29% (20 of 67) reached levels as high as 2.5 to 3. The expression intensity increased in direct association with the tumor grade (see Figure 2).

Association between PKM2 expression and pathologic characteristics. The PKM2 expression intensity was related to the tumor grade (Table 2). The area of positive staining and the intensity of PKM2 expression (mean Q scores) increased in direct proportion to the tumor grade (Figure 3). Among the carcinomas identified as grade 1, 29% (12 of 41), 36% (15 of 41), and 27% (11 of 41) exhibited PKM2 expression scores of 0.5 to 1.0, 1.5 to 2.0, and 2.5 to 3.0, respectively. All tumors with an intensity score of 2.5 to 3.0 were mixed carcinomas. Among the grade 2 carcinomas, nearly 12% (2 of 17) had an expression intensity score of 0.5 to 1.0, over 35% (6 of 17) had a score of 1.5 to 2.0, while nearly 53% (9 of 17) reached a score of 2.5 to 3.0. Likewise, among the grade 3 carcinomas, over 20% (2 of 9) reached an expression intensity score of 1.5 to 2.0 and over 77% (7 of 9) displayed an intensity score of 2.5 to 3.0. PKM2 expression intensity scores also varied among the specific types of carcinoma-tous lesions. The mixed carcinomas typically displayed strong reactivity regardless of tumor grade. No specific relationships were observed between PKM2 expression intensity and any of the other malignancies evaluated.

The expression of HIF1 α also increased in proportion to the tumor grade among the carcinomas, although we found no relationship between HIF1 α expression and the specific type of carcinoma evaluated.

Comparison of PKM2 and HIF1 α expression using qPCR. qPCR was performed to investigate the correlation between the malignancy grade and the expression levels of PKM2 and to determine the relationship between immunohistochemical and molecular findings. Although elevated levels of transcript encoding PKM2 and HIF1 α were detected in neoplastic cells when

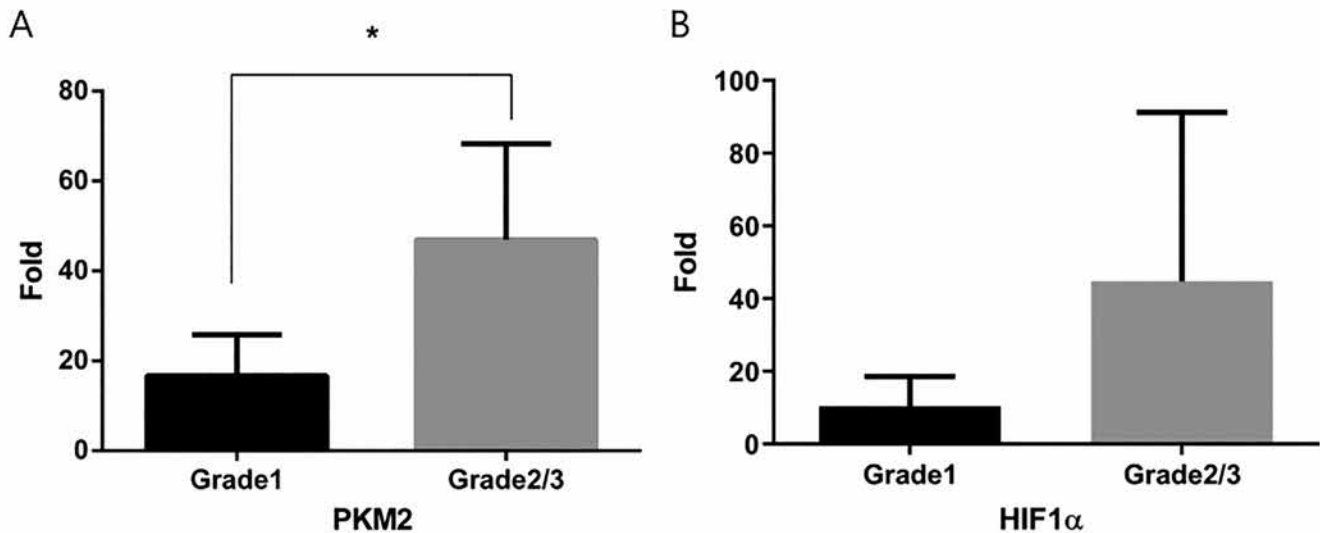


Figure 2. PKM2 and HIF1 α expression by qPCR and tumor grade of canine carcinomas. (A). qPCR detection of PKM2 in canine tumor tissues. (B). qPCR detection of HIF1 α expression in canine tumor tissues. *, $P = 0.0286$.

Table 2. Expression score of PKM2 in canine mammary carcinoma

Score	Grade 1 (n = 41)	Grade 2 (n = 17)	Grade 3 (n = 9)
0	7.3 (3)		
0.5-1	29.2 (12)	11.7 (2)	
1.5-2	36.5 (15)	35.2 (6)	22.2 (2)
2.5-3	26.8 (11)	52.9 (9)	77.7 (7)

Values are either % (n)

compared with normal mammary tissue overall, no significant increases were detected in low-grade tumors. By contrast, cells from grade 2 and 3 tumors expressed much higher levels of PKM2 and HIF1 α than those from grade 1 tumors (Figure 2 A and B). However, the proportionality remains unclear, as expression of transcripts encoding PKM2 in grade 2 tumors was unexpectedly higher than that detected in grade 3 tumors.

Discussion

PKM2, which is transcriptionally induced by HIF1 and interacts with HIF1 α , is considered a new and important target for inhibition of neoplastic growth.⁴ Previous studies have reported high levels of PKM2 expression in association with numerous cancers, including breast, pancreas, colon, renal, liver, testis and lung.^{2,7,8,19,20,22} PKM2 is a known transcriptional target of HIF1 α ;¹⁶ HIF1 α and PKM2 physically interact with one another in the nucleus, which ultimately results in modulation of the transcriptional activity of the HIF1 α gene.¹⁵ This is the first study to present an association between clinicopathological characteristics and the expression of PKM2 and HIF1 α in CMT. Our findings from immunohistochemistry staining and qPCR reveal a positive association between the expression of PKM2 and tumor grade in a study that includes both neoplastic and nonneoplastic mammary tissues.

In the immunohistochemical analysis, HIF1 α was detected at higher levels in tumors than in normal or hyperplastic tissue. Expression of HIF1 α was also associated with tumor grade, specifically among the carcinomas. Hypoxic conditions have been associated with neoplastic metabolism in CMTs as well as in human cancers. Expression of PKM2 in canine tumors was

evaluated to determine if PKM2 is coexpressed at similar levels as those of HIF1 α , and to provide evidence for its potential contributions to the survival of CMT cells via the Warburg effect. PKM2 was detected in a clearly cytoplasmic pattern at various levels of expression. PKM2 levels were higher in tumor cells than in normal or hyperplastic mammary gland tissue. In tumor tissues, the number of positive cells and the intensity of PKM2 expression both increased in association with the tumor grade. Furthermore, PKM2 was detected at high levels in cells from mixed and complex carcinoma tissues, regardless of tumor grade. Both complex and mixed carcinomas include malignant epithelial and benign myoepithelial components, including spindle cells.¹¹ Our analysis revealed PKM2 expression in cells derived from both epithelial and myoepithelial sources.

Others¹² have reported that PKM2 dysregulation led to epithelial–mesenchymal transition (EMT) in human cancer cells. The tumor invasion process includes the migration of cancer cells into the surrounding stroma, which promotes malignant transformation of both epithelial and mesenchymal cells.^{13,25} The EMT characterized for human tumors is similar to that seen in canine mixed and complex carcinomas, and includes neoplastic epithelial and myoepithelial cells. As observed in the EMT associated with human disease, we found high levels of PKM2 in both mixed and complex carcinomas. In our study; the PKM2 levels in both tumors exceeded the level of all other canine carcinomas evaluated. However, we detected PKM2 in the cytoplasmic compartment only as Figure 3 C; in human EMT, PKM2 can also be detected in the cell nucleus.²⁷

Our immunohistochemical analysis found no relationship between the intensity of HIF1 α expression and the specific type of carcinoma, whereas PKM2 was highly expressed in complex and mixed carcinomas, regardless of the tumor grade. This result suggests that PKM2 expression, unlike that of HIF1 α , is activated in tumor cells that originated from both myoepithelial and epithelial cells. Accordingly, PKM2 may be a potential biomarker for EMT, or for tumors originating in myoepithelial cells. The qPCR results revealed expression of transcripts encoding both PKM2 and HIF1 α in tumor tissues at levels that increased in direct association with the tumor grade, although we detected no differences in PKM2 expression between normal tissue and grade 1 tumors. We suspect that PKM2 may display

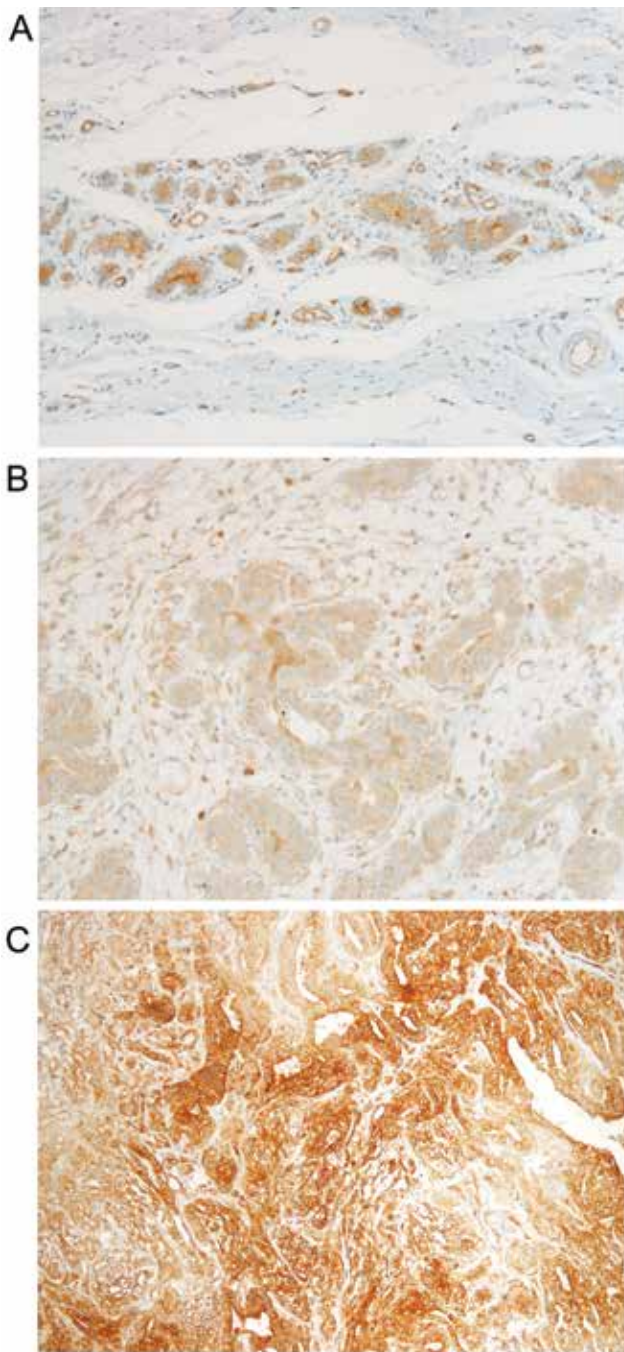


Figure 3. Immunohistochemical detection of PKM2 in canine mammary carcinomas. (A). PKM2 in control mammary tissues ($\times 200$). (B). PKM2 in canine adenoma ($\times 200$). (C). PKM2 in grade 3 complex type canine mammary carcinomas ($\times 200$).

variable expression among the neoplasms evaluated. Our study evaluated only a few of the available tumor samples by qPCR; future work with larger numbers of tumor tissues may be required to demonstrate a relationship between the tumor grade and PKM2 expression.

In conclusion, PKM2 presents a new and important target for controlling tumor metabolism. Our present investigation revealed that PKM2 was expressed in canine mammary carcinoma cells in a pattern similar to that reported in human cancers. Furthermore, our results also suggest that the tumor metabolism in canine tumors may be similar to that identified in human cancers. As such, canine tumors may be an ideal model

for identifying biomarkers and novel therapeutic approaches. We detected expression of PKM2 but not HIF1 α in tumors originating from myoepithelial cells. This result suggests that PKM2 may regulate the metabolism of tumor cells in this unique locale. Further study will be required to uncover the mechanism of PKM2 activation and actions in tumors of myoepithelial origin.

Acknowledgments

This study was supported by the Technology Innovation Program (grant number: 10067737, Establishment of the risk management platform to reduce the attrition of new drugs and their service), was funded by the Ministry of Trade, Industry & Energy (Korea).

References

1. **Abdelmegeed SM, Mohammed S.** 2018. Canine mammary tumors as a model for human disease. *Oncol Lett* **15**:8195–8205. <https://doi.org/10.3892/ol.2018.8411>.
2. **Brinck U, Eigenbrodt E, Oehmke M, Mazurek S, Fischer G.** 1994. L- and M2-pyruvate kinase expression in renal cell carcinomas and their metastases. *Virchows Arch* **424**:177–185. <https://doi.org/10.1007/BF00193498>.
3. **Cazzaniga M, Bonanni B.** 2015. Breast cancer metabolism and mitochondrial activity: the possibility of chemoprevention with metformin. *Biomed Res Int* **2015**:1–9. <https://doi.org/10.1155/2015/972193>.
4. **Chaneton B, Gottlieb E.** 2012. Rocking cell metabolism: revised functions of the key glycolytic regulator PKM2 in cancer. *Trends Biochem Sci* **37**:309–316. <https://doi.org/10.1016/j.tibs.2012.04.003>.
5. **Charafe-Jauffret E, Tarpin C, Bardou VJ, Bertucci F, Ginestier C, Braud AC, Puig B, Geneix J, Hassoun J, Birnbaum D, Jacquemier J, Viens P.** 2004. Immunophenotypic analysis of inflammatory breast cancers: identification of an ‘inflammatory signature’. *J Pathol* **202**:265–273. <https://doi.org/10.1002/path.1515>.
6. **Chen C, Ridzon DA, Broomer AJ, Zhou Z, Lee DH, Nguyen JT, Barbisin M, Xu NL, Mahuvakar VR, Andersen MR, Lao KQ, Livak KJ, Guegler KJ.** 2005. Real-time quantification of microRNAs by stem-loop RT-PCR. *Nucleic Acids Res* **33**:1–9. <https://doi.org/10.1093/nar/gni178>.
7. **Chiavarina B, Whitaker-Menezes D, Martinez-Outschoorn UE, Witkiewicz AK, Birbe R, Howell A, Pestell RG, Smith J, Daniel R, Sotgia F, Lisanti MP.** 2011. Pyruvate kinase expression (PKM1 and PKM2) in cancer-associated fibroblasts drives stromal nutrient production and tumor growth. *Cancer Biol Ther* **12**:1101–1113. <https://doi.org/10.4161/cbt.12.12.18703>.
8. **Christofk HR, Vander Heiden MG, Harris MH, Ramanathan A, Gerszten RE, Wei R, Fleming MD, Schreiber SL, Cantley LC.** 2008. The M2 splice isoform of pyruvate kinase is important for cancer metabolism and tumor growth. *Nature* **452**:230–233. <https://doi.org/10.1038/nature06734>.
9. **DeBerardinis RJ, Lum JJ, Hatzivassiliou G, Thompson CB.** 2008. The biology of cancer: metabolic reprogramming fuels cell growth and proliferation. *Cell Metab* **7**:11–20. <https://doi.org/10.1016/j.cmet.2007.10.002>.
10. **Elston CW, Ellis IO.** 1991. Pathological prognostic factors in breast cancer. I. The value of histological grade in breast cancer: experience from a large study with long-term follow-up. *Histopathology* **19**:403–410. <https://doi.org/10.1111/j.1365-2559.1991.tb00229.x>.
11. **Goldschmidt M, Peña L, Rasotto R, Zappulli V.** 2011. Classification and grading of canine mammary tumors. *Vet Pathol* **48**:117–131. <https://doi.org/10.1177/0300985810393258>.
12. **Hamabe A, Konno M, Tanuma N, Shima H, Tsunekuni K, Kawamoto K, Nishida N, Koseki J, Mimori K, Gotoh N, Yamamoto H, Doki Y, Mori M, Ishii H.** 2014. Role of pyruvate kinase M2 in transcriptional regulation leading to epithelial-mesenchymal transition. *Proc Natl Acad Sci USA* **111**:15526–15531. <https://doi.org/10.1073/pnas.1407717111>.
13. **Hanahan D, Weinberg RA.** 2011. Hallmarks of cancer: the next generation. *Cell* **144**:646–674. <https://doi.org/10.1016/j.cell.2011.02.013>.

14. **Kibbe WA.** 2007. OligoCalc: an online oligonucleotide properties calculator. *Nucleic Acids Res* **35**:W43–W46. <https://doi.org/10.1093/nar/gkm234>.
15. **Luo W, Hu H, Chang R, Zhong J, Knabel M, O’Meally R, Cole RN, Pandey A, Semenza GL.** 2011. Pyruvate kinase M2 is a PHD3-stimulated coactivator for hypoxia-inducible factor 1. *Cell* **145**:732–744. <https://doi.org/10.1016/j.cell.2011.03.054>.
16. **Luo W, Semenza GL.** 2011. Pyruvate kinase M2 regulates glucose metabolism by functioning as a coactivator for hypoxia-inducible factor 1 in cancer cells. *Oncotarget* **2**:551–556. <https://doi.org/10.18632/oncotarget.299>.
17. **Madej JA, Madej JP, Dziegiel P, Pula B, Nowak M.** 2013. Expression of hypoxia-inducible factor-1 α and vascular density in mammary adenomas and adenocarcinomas in bitches. *Acta Vet Scand* **55**:1–7. <https://doi.org/10.1186/1751-0147-55-73>.
18. **Nolan T, Hands RE, Bustin SA.** 2006. Quantification of mRNA using real-time RT-PCR. *Nat Protoc* **1**:1559–1582. <https://doi.org/10.1038/nprot.2006.236>.
19. **Ogawa H, Nagano H, Konno M, Eguchi H, Koseki J, Kawamoto K, Nishida N, Colvin H, Tomokuni A, Tomimaru Y, Hama N, Wada H, Marubashi S, Kobayashi S, Mori M, Doki Y, Ishii H.** 2015. The combination of the expression of hexokinase 2 and pyruvate kinase M2 is a prognostic marker in patients with pancreatic cancer. *Mol Clin Oncol* **3**:563–571. <https://doi.org/10.3892/mco.2015.490>.
20. **Pottek T, Muller M, Blum T, Hartmann M.** 2000. Tu-M2-PK in the blood of testicular and cubital veins in men with testicular cancer. *Anticancer Res* **20**:5029–5033.
21. **Schmittgen TD, Livak KJ.** 2008. Analyzing real-time PCR data by the comparative C(T) method. *Nat Protoc* **3**:1101–1108. <https://doi.org/10.1038/nprot.2008.73>.
22. **Schneider J, Neu K, Grimm H, Velcovsky HG, Weisse G, Eigenbrodt E.** 2002. Tumor M2-pyruvate kinase in lung cancer patients: immunohistochemical detection and disease monitoring. *Anticancer Res* **22**:311–318.
23. **Tiburcio PD, Choi H, Huang LE.** 2014. Complex role of HIF in cancer: the known, the unknown, and the unexpected. *Hypoxia (Auckl)* **2**:59–70. <https://doi.org/10.2147/HP.S50651>.
24. **Untergasser A, Cutcutache I, Koressaar T, Ye J, Faircloth BC, Remm M, Rozen SG.** 2012. Primer3: new capabilities and interfaces. *Nucleic Acids Res* **40**:1–12. <https://doi.org/10.1093/nar/gks596>.
25. **Weinberg RA.** 2008. Mechanisms of malignant progression. *Carcinogenesis* **29**:1092–1095. <https://doi.org/10.1093/carcin/bgn104>.
26. **Wong N, De Melo J, Tang D.** 2013. PKM2, a central point of regulation in cancer metabolism. *Int J Cell Biol* **2013**:1–11. <https://doi.org/10.1155/2013/242513>.
27. **Yang W, Xia Y, Ji H, Zheng Y, Liang J, Huang W, Gao X, Aldape K, Lu Z.** 2011. Nuclear PKM2 regulates β -catenin transactivation upon EGFR activation. *Nature* **480**:118–122. <https://doi.org/10.1038/nature10598>.
28. **Zamani-Ahmadmamdudi M, Nassiri SM, Rahbarghazi R.** 2014. Serological proteome analysis of dogs with breast cancer unveils common serum biomarkers with human counterparts. *Electrophoresis* **35**:901–910. <https://doi.org/10.1002/elps.201300461>.
29. **Zhang Z, Deng X, Liu Y, Liu Y, Sun Y, Chen F.** 2019. PKM2, function and expression and regulation. *Cell Biosci* **9**:1–25. <https://doi.org/10.1186/s13578-019-0317-8>.